ISSN: 0067-2904

Inorganic Geochemistry and Origin of Bitumen Intruded in Euphrates and Fatha Formations in Hit Area, Western Iraq

Salih Muhammad Awadh[1*], Zinah Saleem Al-Ankaz[2]

[1]Department of Geology, College of Science, University of Baghdad, Baghdad, Iraq
[2]Department of Physics Science, College of Science, University of Wasit, Wasit, Iraq

Abstract

The content of redox sensitive trace element (V, Co, Ni, and Mo) in the bituminous limestone of the Euphrates Formation (E. Miocene) and bituminous gypsum of the Fatha Formation (M. Miocene) in the Hit Abu-Jir village area, Anbar governorate were determined using Inductively-Coupled Plasma Mass Spectrometer (ICP-MS), in order to infer the origin of the hydrocarbon and the depositional conditions of the organic matter. Hydrocarbons species by using FTIR technique was identified as aliphatic, aromatic compound, hydroxyl acids, hydroxyl group, sulfoxide and sulfur. Bitumen occurrences in these formations is a result of the hydrocarbon seepages that moved up under high pressure along the Abu-Jir fault Zone, and then were intruded in the limestone and gypsum beds of Euphrates and Fatha Formations. A distinctive fractional differentiation in trace elements in the hydrocarbon-bearing fluids was detected, and resulted in enrichment of these trace elements in the carbonates of the Euphrates, rather than in gypsum belonging to the Fatha. The source of the organic matters located in the Euphrates carbonates is mainly marine planktonic deposited in an anoxic environment, whilst, for that located in the gypsum of Fatha Formation is marine anoxic carbonate-shale, marine terrestrial oxic-dysoxic, and terrestrial oxic. The original kerogen is estimated as of type- I/ II. Bitumen precipitated in shallow depth does not exceed 2 km. The temperature of the ascending hydrocarbons-bearing fluids is computed as 35°C, whereas the burial depth is of 61°C, where the biodegradation was the most probable process responsible for producing bitumen in such depth and temperature.

Keywords: Hydrocarbons, FTIR, Bitumen, Euphrates Formation, Fatha formations

الجيوكيمياء اللاعضوية وأصل البتيومين المقحم في تكويني الفرات والفتحة في منطقة هيت ،غرب العراق

صالح محمد عوض[1*]، زينة سليم العنكز[2]

[1]قسم علم الارض، كلية العلوم، جامعة بغداد، بغداد، العراق
[2]قسم علوم الفيزياء، كلية العلوم، جامعة واسط، واسط، العراق

الخلاصة

تم تحديد محتوى العناصر النزرة(الفناديوم ، النيكل ،الكوبلت و المولبدنيوم) الحساسة للبيئة الاختزالية في صخور الحجر الجيري البتيوميني لتكوين الفرات (المايوسين المبكر) و صخور الجبسم البتيوميني لتكوين الفتحة (المايوسين المتوسط) في منطقة هيت–ابو جير، محافظة الانبار. حيث تم تحديد العناصر النزرة

---

* Email: salihauad2000@yahoo.com

باستخدام جهاز المطياف الكتلي البلازمي الحثي، وذلك لتحديد اصل الهيدروكربونات و بيئة ترسيب المادة العضوية. تم تحديد انواع الهيدروكربونات باستخدام جهاز قياس طيف الاشعة تحت الحمراء حيث شخصت مركبات اليفاتية، اروماتية، احماض هيدروكسيلية، مجموعة الهيدروكسيل وأكاسيد كبريتية و كبريت. يوجد البتيومن ضمن هذه التكاوين نتيجة حركة الهيدروكربونات تحت ضغط عالي باتجاه الاعلى على امتداد نطاق فالق ابو جير، والتي بعد ذلك اقحمت في طبقات الصخور الجيرية لتكوين الفرات والصخور الجبسية لتكوين الفتحة. تم التحسس بحصول تجزئة تفاضلية مميزة للعناصر النزرة في الموائع الحاملة للهيدروكربونات، نتج عن ذلك اغناء بالعناصر النزرة للصخور الكربونايتية العائدة لتكوين الفرات على حساب الصخور الجبسية لصخور الفتحة. ان اصل المواد العضوية في الصخور الكربوناتية لتكوين الفرات هو الكائنات الدقيقة العالقة ذات الاصل البحري و المترسبة في بيئة لاهوائية. اما المواد العضوية في الصخور الجبسية لتكوين الفتحة فهي ذات اصل بحري كربونايتي الى سجيلي مترسب في بيئة مختلطة بحرية غير مؤكسجة، خليط من بيئة بحرية وقارية مؤكسجة و قارية مؤكسجة. تم تحديد نوع الكيروجين الاولي على انه يعود الى نوع 1 ونوع 2. ترسب البتيومن في عمق ضحل لا يتجاوز 2 كم. تم حساب درجة حرارة المحاليل الصاعدة الحاملة للهيدروكربونات لتكون 35^o درجة مئوية بينما درجة حرارة عمق الطمر الذي يتواجد عنده البتيومن هي 61 درجة مئوية، حيث يعتقد في الغالب ان عملية التحلل الاحيائي هي المسؤولة عن انتاج البتيومن في مثل هذا العمق وهذه الحرارة.

Introduction

Hydrocarbons seepages (bitumen and H_2S gas) are distinct phenomenon can be easily seen on surface at the western side of the Euphrates River, particularly, in area extended between Hit and Abu-Jir village [1].Some seepages associate the sulfurous spring water, while others are independent bitumen seeps Figure-1. These seepages reflect the NW-SE trend of the Abu-Jir Fault Zone (AJFZ). The interaction among Abu-Jir Fault Zone with Euphrates and Fatha basins appears as bitumen seepages and sulfurous water springs as evidence for recent activity along Anah-Abu Jir Fault [2]. Oil seeps were generated from planktonic kerogen partially mixed with the terrestrial material belong to source rock older than Jurassic and Cretaceous rocks [3]. These seeps are characterized by non-waxy oil originated from the marine organic source deposited under anoxic conditions [3]. The abundance of trace elements in the crude oils and bitumen have a wide range varies from less 1ppb to more than several thousand ppm [4]. Nickel (Ni) and vanadium (V) occur in oils and bitumen as metallo-porphyrins and non-porphyrin species; they are usually the most abundant metals with values ranging up to 200 ppm Ni and 2000 ppm V [4]. The relative concentrations of some trace elements such as Ni and V are generally resistant to hydrocarbon maturity, secondary alteration and unaffected by hydrocarbon migration [5], [6] and [7]. Therefore, these metals are used as geochemical indicators of source rocks, paleo-depositional environment and organic facies. In the current study trace element geochemistry and FTIR technique were used to identify the origin of bitumen, depositional setting of organic input, parent kerogen type and paleo-temperature.

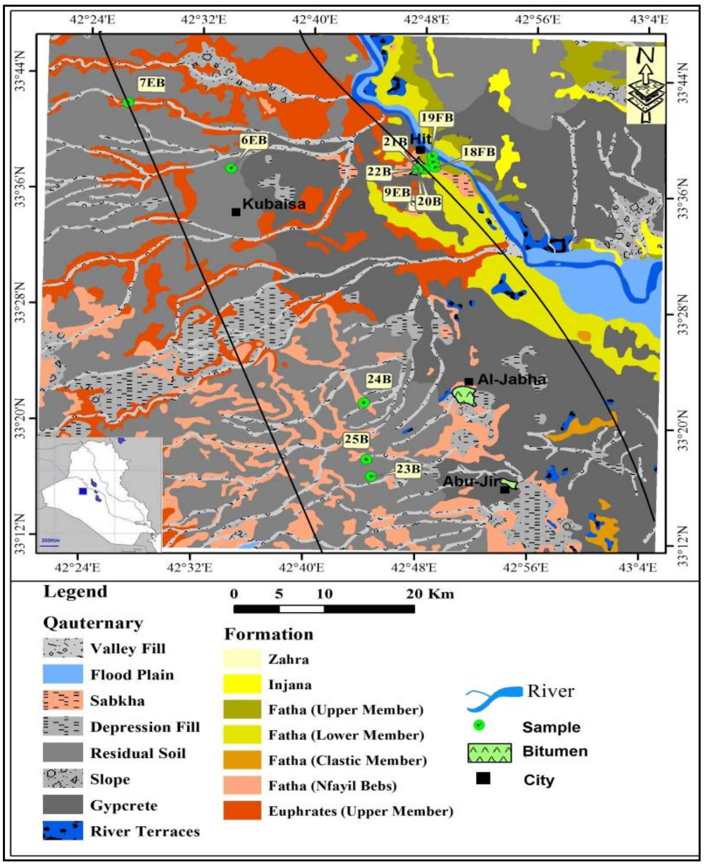

Figure 1- Geological and locational map of the study area displays sampling sites along the AJFZ (after [8]).The approximate boundary of AJFZ installed in this map based on [1].

Materials and methods

Sixteen samples (five bituminous limestone and eleven bituminous gypsum samples) were collected from the area between Hit and Abu-Jir village Figure-1. Samples (6EB to 19FB) represent a partially impregnated with bitumen. So, the bitumen-saturated fraction was carefully separated from whole rock. Samples from 20B to 25B represent bituminous gypsum rocks that were wholly impregnated with bitumen. All samples were subjected to Inductively Coupled Plasma technique (ICP) at the ALS Laboratory Group, SL- Seville in Spain. A total of ten samples are selected for the investigation by the Fourier Transform Infrared Spectrophotometry (FTIR), Shimadzu instrument at the Environmental Laboratory University of Baghdad to identify the hydrocarbon species of bitumen impregnated in limestone and gypsum samples. Geological map and sampling site was drawn using GIS software.

Results and discussion

Source rocks and paleo-depositional environment

The non-porphyrin Ni and V complexes in the crude oil form may be primary or secondary. The metal complexes released from kerogen during catagenesis and formation of metal-organic complexes represents primary origin, whilst secondary includes the metallic complexes derived via the interaction of oils with sediments or waters during migration and maturation. Biodegradation may also affect the concentrations of some trace elements in crude oils [4]. The results of the element concentrations (V, Co, Ni and Mo) and their ratios are listed in Table-1. The concentration averages of V, Co, Ni and Mo in the bituminous limestone of the Euphrates Formation (41.2, 5.8, 43.8 and 5.2 ppm) are clearly more than of those in the bituminous gypsum of Fatha Formation (33, 1.0, 38, and 1.0 ppm).The depletion of trace elements in the bituminous gypsum of Fatha Formation could be attributed to incorporate the largest content of these trace elements in calcite lattice of Euphrates Formation leaving trace elements-poor fluid. So, the remnants trace elements were incorporated within gypsum lattice which belongs to the Fatha Formation. Accordingly, when using the cross plot of V versus Ni proposed by [9],[5], [10]and [11] Figure-2.

The majority of the bitumens gypsum samples are plotted in the marine anoxic zone Figure-2 with the exception of one sample that plot in the marine–anoxic–carbonatic shale. So, the Euphrates bitumen was mainly sourced from marine rocks that were deposited in an anoxic environment. It may seem, bitumen in gypsum of Fatha Formation appears as of different origin (marine anoxic carbonatic-shale, marine terrestrial oxic-dysoxic, and terrestrial oxic Figure-2. Redox sensitive parameters including V/Ni, V/(V+Ni) and Ni/Co are most widely used in hydrocarbon–source correlations; because, these ratios vary significantly in different sedimentary settings and generally not influenced by reservoir mineralogy or fluid migration [12] [13]. [11],[5] and [14proposed that bitumen deposited in reducing environments has a V/Ni ratio more than 3.0. The V/Ni ratio higher than 3 indicates marine organic material, ranging from 1.9 to 3 indicates mixed terrigenous and marine source input, less than 1.9 indicates predominantly terrigenous organic materials. The V/Ni ratio in the bituminous carbonates varies between (0.41-5.1) while in evaporites ranges between (0.8-6.5). It is clear, bitumen is of wide range of V/Ni ratio. So, the mixed marine and terrigenous source input is suggested.[15] proposed the following values and conditions for the ratio V/(V+Ni): the ratio that are more than 0.84 reflect euxinic, 0.54–0.82 is anoxic, where 0.46–0.60 are suggestive of dysoxic conditions. Also the ratio Ni/Co; more than 7.0, 5.0–7.0 and less than 5.0 indicates anoxic, dysoxic and oxic environments, respectively [15]. Accordingly, the vast majority of the Euphrates samples (EB) have Ni/Co ratio, where the average of Ni/Co is 8.57 indicate an anoxic environment. The ratio Ni/Co in most samples of the Fatha Formation (FB) is lower than of 7, where it is 7 in sample 17 FB and 11 in sample 18FB. However, the average of Ni/Co (8.8) indicates anoxic environment. [10] proposed values of V/Ni ratio to identify the precursor of organic materials.

Table 1- Results of some redox sensitive trace elements and their ratios in the sedimentary bituminous rocks.

Sample No.		V	Co	Ni	Mo	V/Ni	V/V+Ni	Ni/Co
		ppm						
Euphrates Formation	6EB	18	4.0	43	2.0	0.41	0.30	10.75
	7EB	39	6.0	52	6.0	0.75	0.42	8.66
	8EB	77	9.0	15	6.0	5.1	0.83	1.66
	9EB	37	5.0	53	4.0	0.7	0.41	10.6
	10EB	35	5.0	56	8.0	0.62	0.38	11.2
	Mean	**41.2**	**5.8**	**43.8**	**5.2**	**1.5**	**0.46**	**8.57**
Fatha Formation	15FB	17	1.0	3.0	1.0	5.6	0.85	3.0
	16FB	17	1.0	5.0	1.0	3.4	0.77	5.0
	17FB	12	1.0	7.0	1.0	1.7	0.63	7.0
	18FB	9.0	1.0	11	1.0	0.8	0.45	11
	19FB	5.0	1.0	1.0	1.0	5.0	0.83	1.0
	20B	32	1.0	6.0	1.0	5.3	0.84	6.0
	21B	39	1.0	6.0	1.0	6.5	0.86	6.0
	23B	55	1.0	13	1.0	4.2	0.81	13
	24B	110	1.0	28	1.0	3.9	0.81	28
	Mean	**33**	**1.0**	**8.8**	**1.0**	**4.0**	**0.76**	**8.8**

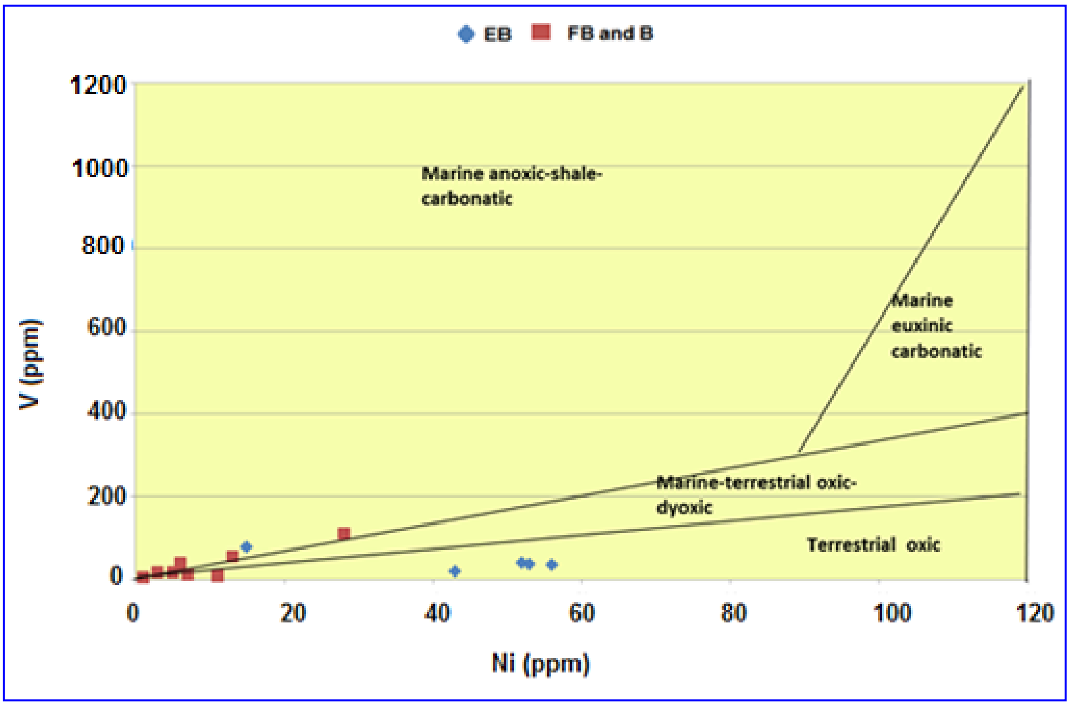

Figure 2- Cross plot of V versus Ni concentrations indicate the redox conditions in the depositional environment of the source rocks after [9],[5], [10] and[11]. EB bituminous carbonate rocks, FB and B bituminous gypsum rocks.

Hydrocarbon species

FTIR spectra identification was done based on the spectra standard table Table-2. Bitumens that were intruded limestone and gypsum are composed of aliphatic, and aromatic compounds containing hydroxyl group, hydroxyl acids, sulfoxide and sulfur. These hydrocarbon compounds are incorporated in limestone and gypsum. A total of ten samples of bituminous carbonate and gypsum rocks were chosen (three bituminous carbonates and seven bituminous gypsum). Distinctive IR spectra of hydrocarbon species were identified Figurs- 3, 4 and 5. The FTIR spectra of bituminous carbonates revealed that many hydrocarbon species are incorporated with calcite in samples 6EB and 7EB), whereas the sample (8EB) is wholly consisted of hydrocarbons Figure- 3. The bituminous gypsum (19FB, 20B, 21B, 22B and 23B) have striking peaks of hydrocarbon species and traces of gypsum, while IR spectra of gypsum in the samples 24B and 25B disappeared due to complete impregnation by bitumen Figure-5.

Table 2- Spectra standard table of the minerals and organic compound types

Bond	**Minerals and organic compound Types**	**Wavelength range (cm^{-1})**	**Intensity**	**References**
C-O in CO_3	Calcite	1798 1429-1453 848-877 713-720	Strong Medium Weak Weak	[16] and [17]
H-O-H O-H S-O S-O	Gypsum	3547.09-3404.36 1687,1622 1141.95-1116.78 669.3- 601.79	Strong Medium Strong Weak	[18]
O-H	Hydroxyl group	3600-3645	Medium	[19] and[20]
C-H	Aliphatic alkane alkyl	2950-2970 2860-2880	Medium	
C≡C	Medial alkyne	2190-2260	Medium-weak	
C=C	Aromatic combination Bands (Alkene)	1600-2000	Medium-weak	

C-H	Aromatic (Alkene)	1410-1420	Medium	
C=O	Carbonyl Carboxylic acids	1700 1690	Strong Medium	
C-O	C-O bond in bitumen structure	1078-1300	Medium- weak	
S=O	Sulphoxide	1032-1042	Strong-medium	
C-H	Aromatic(Alkyne)	610–680	Weak	
S-S and/or C-S	Sulfur	500-700	Medium-weak	[21] (2013)

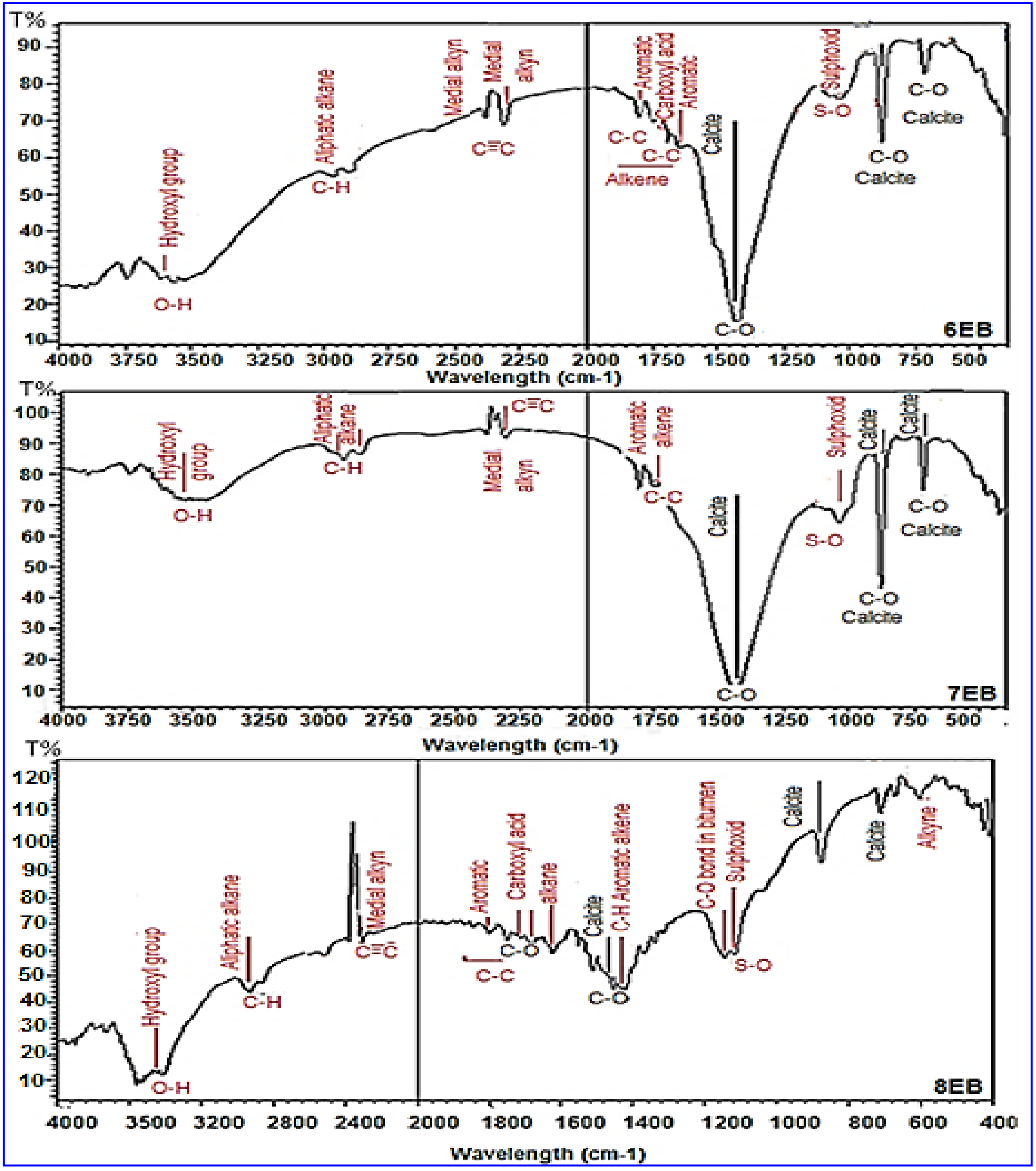

Figure 3- FTIR spectra diagram of the bituminous carbonates (6EB, 7EB and 8EB) in the Euphrates Formation.

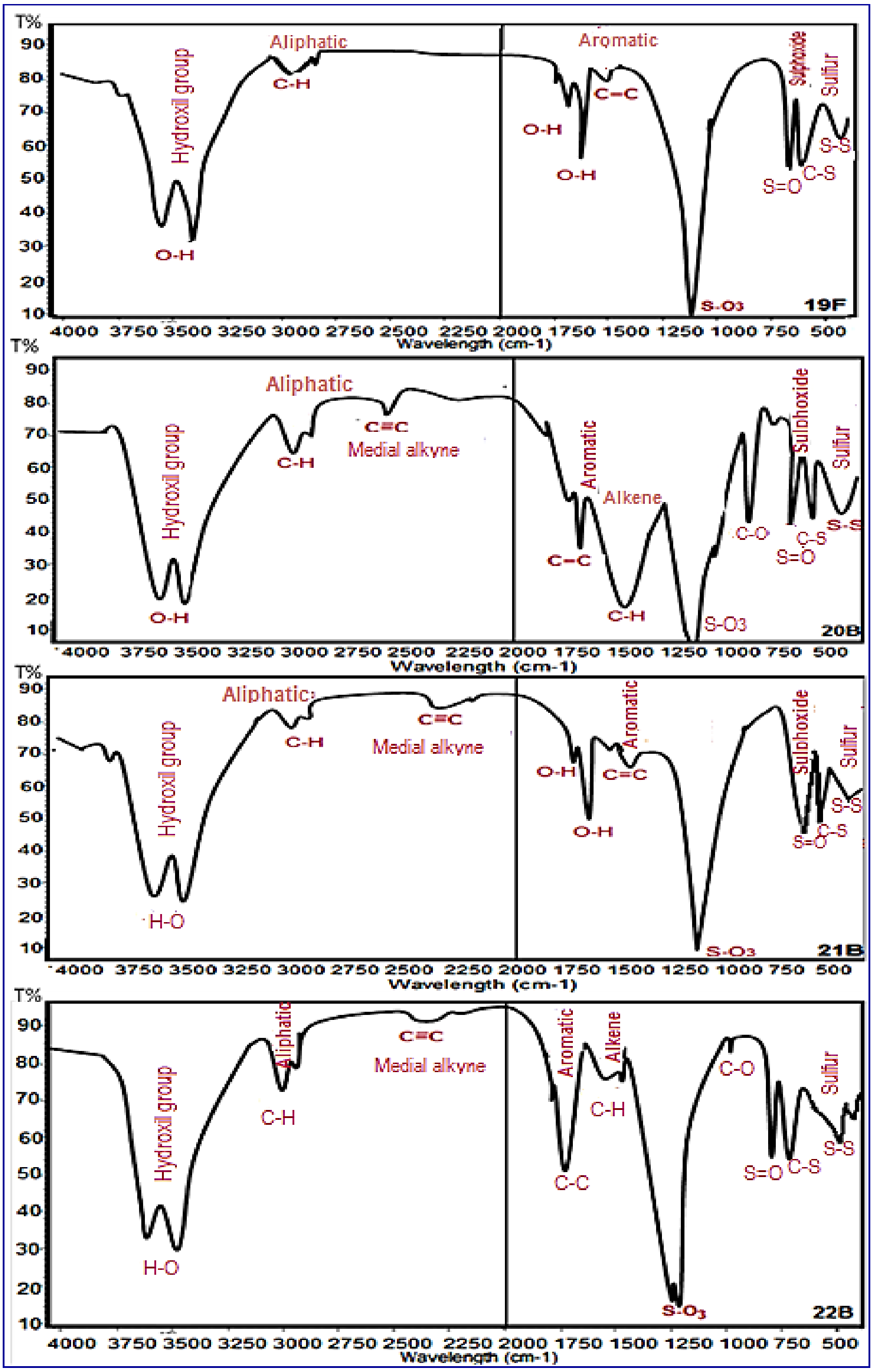

Figure 4- FTIR spectra diagrams of bituminous gypsum samples (19FB,20B, 21B and 22B) in the Fatha Formation.

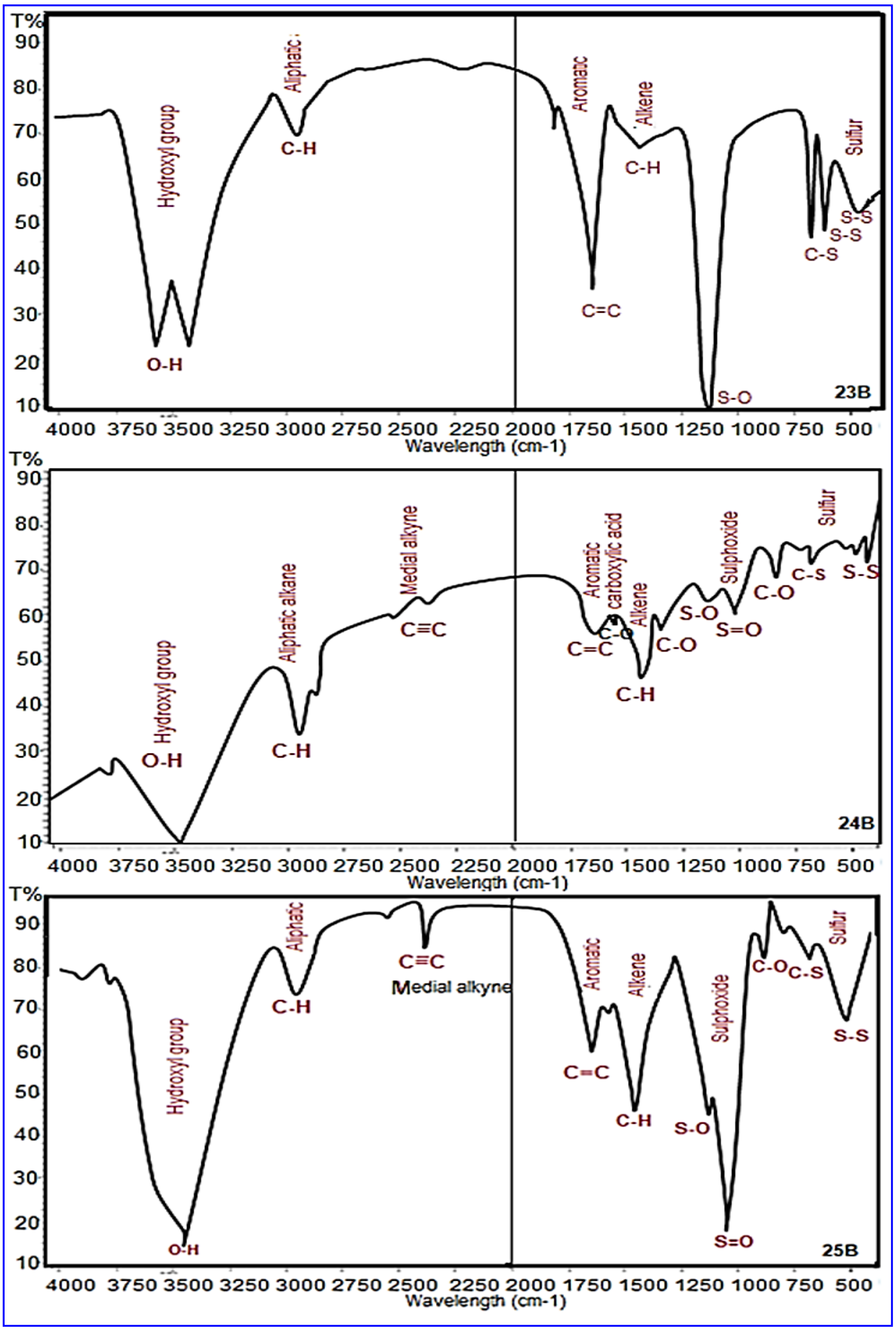

Figure 5- FTIR spectra diagrams of bituminous gypsum samples (23B, 24B and 25B) in the Fatha Formation.

The kerogen type and paleotemperature

FTIR technique was used to determine the parent kerogene type and vitrinite reflectance. The vitrinite reflectance is used to estimate the burial temperature when bitumen precipitated ($T_{peak\ burial}$) and the temperature of oil field fluids ($T_{peak\ fluids}$). Paleo-temperature estimation is important to predicate the processes by which oil alters to bitumen again and to estimate the depth of bitumen after the precipitation. The classification plot of organic matter types proposed by [22] and [23] was adopted. The classification plot of organic matter types and maturation is based on A-Factor and C-Factor [22] and [23]. This plot is comparable to the van Krevelen diagram Figure-6. A- Factor and C-Factor obtained from the IR spectra diagram.

$$\text{A-Factor} = (2860 + 2930cm^{-1})/(2860 + 2930 + 1630cm^{-1})\ldots (1)$$

$$\text{C-Factor} = (1705cm^{-1})/(1705 + 1630cm^{-1}) \ldots (2)$$

The transmittance spectra of aliphatic groups typically display distinctive peaks at 2860 and 2930 cm^{-1} wavelength, carboxyl and carbonyl groups at 1705 cm^{-1} and at 1630 cm^{-1} wavelength, aromatic C=C bands. Each wavelength on the X axis of IR spectra diagram has equivalent value (Ev) on Y axis(T%); these values (Ev) when applied in equation of A-Factor and C-Factor will give relative ratios of the intensities of aliphatic/aromatic bands and ratios of carboxyl and carbonyl/aromatic bands respectively[24].The equivalent values (Ev) are listed in Table- 3. With increasing maturation the aliphatic peaks initially increase, while the carboxyl/carbonyl peak decreases. As maturation continues to increase, the aliphatic peaks decrease, while there is no apparent change in the peaks representing the aromatic C=C bands. Plotting the relative ratios of the intensities of aliphatic/aromatic bands (A-Factor) against the ratios of carboxyl and carbonyl/aromatic bands (C-Factor) in a classification plot Figure- 6 results in an excellent differentiation of the organic matter.

One of most important features of this classification plot, is allowing the precise determination of vitrinite reflectance (Ro%) [25] Bituminous samples have striking peaks of aliphatic and aromatic spectra (Figures-3, 4 and 5). A and C-Factors values of each sample was applied in Figure-6. Each sample had certain site on vitrinite reflectance equivalent grid reflects each sample (Ro%) value Table-3. Bitumen appears to be derived from lacustrine and marine planktonic kerogen of type- I and II. Kerogen type I is highly oil-prone, yielding high quantities of paraffinic hydrocarbons, while type II is moderate oil-prone [26].

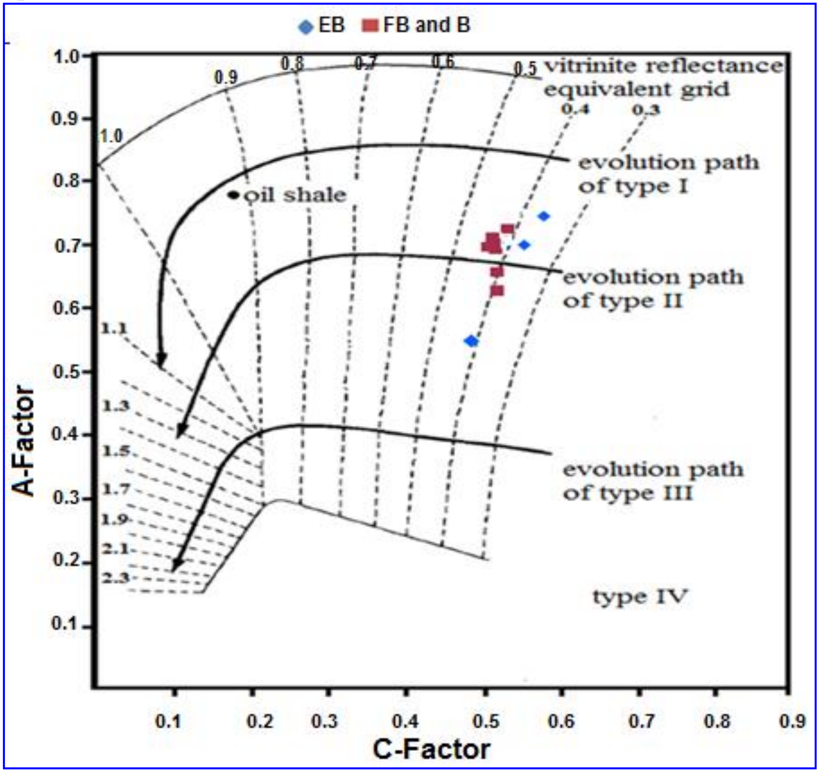

Figure 6 - Classification plot of organic matters types and maturation (figure after[22] and [23]).

Some of the previous studies mentioned, that the Palaeotemperature can be estimated by illite crystallinity, fluid inclusion homogenization temperature and vitrinite reflectance [27]. In the current study, the vitrinite reflectance was used. Vitrinite reflectance (Ro%) data Table- 3 can in turn be used to estimate peak temperature (T_{peak}) by a calibrated vitrinite reflectance geothermometer (VRG) of [28]. The equations are:

$$T_{peak\ fluids} = [\ln(Ro\%) + 1.19]/0.00782\ldots(3)$$

Consequently, the T $_{peak\ fluids}$ was 35°C in average which represents the oil field fluids temperature within the sedimentary basin.

$$T_{burial} = [\ln(Ro\%) + 1.68]/0.0124\ldots(4)$$

Table 3- The equivalent values (Ev) values, A and C-Factors, vitrinite reflectance (Ro%),temperatures of fluids(T°C fluids) and temperatures of burial (T°C burial) in the bituminous samples.

Sample no.		**Ev (2860)**	**Ev (2930)**	**Ev (1630)**	**Ev (1705)**	**C-Factor**	**A-Factor**	**Ro%**	**T°C fluids**	**T°C burial**
Euphrate Formatio	6EB	49.4	48.3	79.7	77.7	0.49	0.55	0.41	38	63.5
	7EB	92.9	90.1	55.2	66.4	0.54	0.76	0.38	28.4	57.4
	8EB	54.6	48.5	44.3	48.2	0.52	0.69	0.39	31.7	59.5
Fatha Formation	19FB	84.7	81.5	86.7	86.9	0.50	0.65	0.40	35	61
	20B	83.1	80.4	58.9	63.7	0.51	0.73	0.40	35	61
	21B	91.6	88.1	83.5	84.0	0.50	0.68	0.40	35	61
	22B	80.9	79.5	78.9	80.6	0.50	0.67	0.40	35	61
	23B	83.6	82.7	81.4	80.4	0.49	0.67	0.41	38	63.5
	24B	59.7	56.9	67.7	73.2	0.51	0.63	0.40	35	61
	25B	81.8	83.6	85.9	83.3	0.49	0.65	0.41	38	63.5
Mean								0.40	35	61

Also, the T $_{peak\ burial}$ was computed to be 61°C representing the burial temperature of bitumen precipitated. Hence, in depending on the temperature values, bitumen-bearing oil was intruded Euphrates and Fatha Formations in shallow depth not more than 2 km depend on geothermal gradient. Such these values of temperatures (35°C of fluid and 61°C of burial depth) are not sufficient to alter oil to bitumen by thermal cracking, but biodegradation is the most effective process in this depth and temperature. The biodegradation is the microbial oxidation of crude oil controlled by temperature less than 80°C [29].

Conclusions

The hydrocarbons- bearing fluids were rich in sensitive redox trace elements (V, Co, Ni and Mo). A distinctive fractional differentiation in trace element concentrations was detected. The large content of the total trace element concentrations were incorporated in the carbonates of the Euphrates Formation, consequently, the remnant hydrocarbons- bearing fluids become depleted in the trace elements. Thereafter, the depleted fluids intruded gypsum rocks of Fatha Formation; and so, the trace element concentrations in the gypsum are few.

Aliphatic and aromatic compounds linked with hydroxyl group, hydroxyl acids, sulfoxide and sulfur are the major components of the bitumen. In depending of the redox sensitive element concentrations, the bitumen that was intruded both of the Euphrates and Fatha Formations is of different sources. Organic matters that ascended and situated in the Euphrates carbonates were mainly sourced from marine planktonic that were deposited in an anoxic environment whereas organic matters that situated in the gypsum of Fatha Formation were originated from multi sources (marine anoxic carbonate-shale, marine terrestrial oxic-dysoxic, and terrestrial oxic). The parent kerogen is estimated as of type- I/ II.

Bitumen precipitated in shallow depth not exceed 2 Km. The temperature of the ascending hydrocarbons-bearing fluids is computed as 35°C, whereas the burial depth is 61°C. Biodegradation was the most probable process responsible for producing bitumen in such depth and temperature.

References

1- Awadh, S. M., Ali, K. K., and Alazzawi, A. T. **2013**. Geochemical exploration using surveys of spring water, hydrocarbon and gas seepage, and geobotany for determining the surface extension of Abu-Jir Fault Zone in Iraq: A new way for determining geometrical shapes of computational simulation models. *Journal of Geochemical Exploration*, 124, pp: 218–229.

2- Sissakian, V. K. and Deikran, D. B. **2009**. Neotectonic movements in West of Iraq. *Iraqi Bulletin of Geology and Mining*, 2, pp: 51-124.

3- Awadh, S. M. and Hussien, S. A. **2015**. Organic Geochemistry and Stable Carbon Isotopes of Oil Seepages in the Abu-Jir Fault Zone at Al-Anbar Governorate. *Iraqi Journal of Science*, 56, pp: 3162-3175.

4- Fibly, R. H. **1994.** Origin and nature of trace element species in crude oils, bitumens and kerogens: implications for correlation and other geochemical studies. *Geological Society*, London, Special Publications, 78, pp: 203-219.

5- Lewan, M.D. **1984**. Factors controlling the proportionality of vanadium to nickel in crude oils. *Geochimica Cosmochimica*, 48, pp: 2231–2238.

6- Lopez, L., Lonaco, S., Galarraga, F., Lira, A. and Cruz, C. **1995**. V/Ni ratio in maltene and asphaltene fractions of crude oils from the west Venezuelan basin: Correlation studies. *Chemical Geology*, 119, pp: 255–262.

7- Wilde, P., Lyons, T.W. and Quinby-Hunt, M.S. **2004.** Organic carbon proxies in black shales: Molybdenum. *Chemical Geology*, 206, pp: 167–176.

8- Iraq Geological Survey. **1995**. Geological Map of Al-Ramadi Quadrangle, Sheet NI-38-9. 1:100 000 quaderanles. Geoserv, Baghdad, Iraq.

9- Lewan, M.D. and Maynard, J.B. **1982.** Factors controlling enrichment of vanadium and nickel in the bitumen of organic sedimentary rocks. *Geochimica Cosmochimica*, 46, pp: 2547–2560.

10- Galarraga, F., Llamas, J.F., Martïnez, A., Martnez, M., Flamas, J.F. and Mrquez, G. **2008.**V/Ni ratio as a parameter in palaeoenvironmental characterization of nonmature medium-crude oils from several Latin American basins. *Journal of Petroleum Science and Engineering*, 61, pp: 9–14.

11- Akinlua, A., Adekola, S.A., Swakamisa, O., Fadipe, O.A. and Akinyemi, S.A. **2010**. Trace element characterisation of Cretaceous Orange basin hydrocarbon source rocks. *Applied Geochemistry*, 25, pp: 1587–1595.

12- Lopez, L., Lo Monaco, S. and Richardson, M. **1998.** Use of molecular parameters and trace elements in oil–oil correlation studies, Barinas sub-basin, Venezuela. *Organic Geochemistry*, 29, pp: 613–629.

13- Lopez, L. and Lo Monaco, S. **2004.** Geochemical implications of trace elements and sulfur in the saturate, aromatic and resin fractions of crude oil from the Mara and Mara Oeste fields. *Venezuela Fuel*, 83, pp: 365–374.

14- Quinby-Hunt, M.S. and Wilde, P. **1994**. Thermodynamic zonation in the black shale facies based on iron-manganese-vanadium content. *Chemical Geology*, 113, pp: 297–317.

15- Hatch, J.R. and Leventhal, J.S. **1992**. Relationship between inferred redox potential of the depositional environment and geochemistry of the Upper Pennsylvanian (Missourian) stark shale member of the Dennis limestone, Wabaunsee country, Kansas, USA. *Chemical Geology*, 99, pp: 65–82.

16- Adler H.H. and Kerr P.F. **1962.** Infrared study of aragonite and calcite. *American Mineralogist*, 47, pp: 700-717.

17- Jones G. C. and Jackson. B. **1993**. *Infrared Transmission Spectra of Carbonate Minerals*. First edition. Natural History Museum, London, 233p.

18- Salisbury, J. W., Walter L. S. and N. Vergo. **1987**. Mid-infrared (2.1–25 mm) spectra of minerals. First edition, U.S. *Geological survey*. Open file report. pp: 87–263.

19- Nciri N, Song S, Kim N. and Cho N. **2014**. Comparison of Chemical Properties of Trinidad Lake Asphalt and Asphalt Ridge bitumen. (Under publication).

20- Coates. J. and Wiley. O. **2000**. Interpretation of Infrared Spectra, A Practical Approach. *In Encyclopedia of Analytical Chemistry*, pp: 10815–10837.

21- Isayev, A.I. **2013**. *The Science and Technology of Rubber*. 4th edition. Boston. Academic Press, pp: 697–764.

22- Ganz, H. and Robison, V. D. **1985**. Newly developed infrared method for characterizing kerogen type and thermal maturation. *Organic geochemistry*.96, pp: 16-20.

23- Ganz, H. **1986**. Organic and inorganic chemical investigations Egyptian black shales. Phosphorus equal complements method development and genetic model. *Berlin geowiss,* 94, pp: 70-113.

24- Ganz, H. and Kalkreuth, W. **1991**. IR classification of kerogen type, thermal maturation, hydrocarbon potential and lithological characteristics. *Journal of Southeast Asian Earth Sciences,* 5, pp: 19-28.

25- Ganz, H. **1987**. Geochemical evaluation of hydrocarbon source rock characteristics and facies analysis methods and application. *Berliner geowiss*,75, pp: 669-90.

26- Ruiz, S. I. and Crelling, C. J. **2008**. *Applied Coal Petrology*, first edition, Elsevier Ltd. 388p.

27- Barker, C.E. and Goldstein, R.H., **1990.** Fluid-inclusion technique for determining maximum temperature in calcite and its comparison to the vitrinite reflectance geothermometer. *Geology,* 18, pp: 1003-1006.

28- Barker, C.E. and Pawlewicz, M.J. **1994**. Calculation of vitrinite reflectance from thermal histories and peak temperatures، A comparison of methods, in Mukhopadhyay, P.K and Dow, W.G. Vitrinite reflectance as a maturity parameter; Applications and limitations: Washington, D. C. *American Chemical Society,* pp: 216–229.

29- Larter, S.R., Huang, H., Adams, J., Bennet, B., Jokanola, O., Oldenburg, T., Jones, M., Head, I.M., Riediger, C.L. and Fowler, M. **2006**.The controls on the composition of biodegraded oils in the deep subsurface: Part II - Geological controls on subsurface biodegradation fluxes and constraints on reservoir-fluid property prediction. *AAPG Bulletin,* 90(6), pp: 921-938.

30- Head, I.M., Jones, D.M., Larter, S.R., **2003.** Biological activity in the deep subsurface and the origin of heavy oil. *Nature,* 426, pp: 344-352.

31- Roadifer, R.E. **1987**. Exploration for heavy crude oil and natural bitumen, *Petrolum geology*, 1, pp: 3-23.